

Primitive Simultaneous Optimization of Similarity Metrics for Image Registration

Diana Waldmannstetter^{1,2*}, Benedikt Wiestler³, Julian Schwarting³, Ivan Ezhov^{1,4}, Marie Metz³, Spyridon Bakas^{5,6,7}, Bhakti Baheti^{5,6,7}, Satrajit Chakrabarty⁸, Daniel Rueckert^{9,10}, Jan S. Kirschke³, Rolf A. Heckemann¹¹, Marie Piraud¹², Bjoern H. Menze^{2†}, and Florian Kofler^{1,3,4,12†}

- ¹ Department of Informatics, Technical University of Munich, Munich, Germany
² Department of Quantitative Biomedicine, University of Zurich, Zurich, Switzerland
³ Department of Diagnostic and Interventional Neuroradiology, School of Medicine, Klinikum rechts der Isar, Technical University of Munich, Munich, Germany
⁴ TranslaTUM - Central Institute for Translational Cancer Research, Technical University of Munich, Munich, Germany
⁵ Center for Artificial Intelligence and Data Science for Integrated Diagnostics (AI2D) and Center for Biomedical Image Computing and Analytics (CBICA), University of Pennsylvania, Philadelphia, PA, USA
⁶ Department of Pathology and Laboratory Medicine, Perelman School of Medicine, University of Pennsylvania, Philadelphia, PA, USA
⁷ Department of Radiology, Perelman School of Medicine, University of Pennsylvania, Philadelphia, PA, USA
⁸ Department of Electrical and Systems Engineering, Washington University in St. Louis, St. Louis, MO, USA
⁹ Artificial Intelligence in Healthcare and Medicine, Technical University of Munich, Munich, Germany
¹⁰ Department of Computing, Imperial College London, London, U.K.
¹¹ Department of Medical Radiation Sciences, University of Gothenburg, Gothenburg, Sweden
¹² Helmholtz AI, Helmholtz Zentrum München, Munich, Germany

Abstract. Even though simultaneous optimization of similarity metrics is a standard procedure in the field of semantic segmentation, surprisingly, this is much less established for image registration. To help closing this gap in the literature, we investigate in a complex multi-modal 3D setting whether simultaneous optimization of registration metrics, here implemented by means of primitive summation, can benefit image registration. We evaluate two challenging datasets containing collections of pre- to post-operative and pre- to intra-operative Magnetic Resonance (MR) images of glioma. Employing the proposed optimization, we demonstrate improved registration accuracy in terms of *Target Registration Error (TRE)* on expert neuroradiologists' landmark annotations.

Keywords: Registration · Brain Tumor · Similarity Metric · Loss Function · Glioma

*diana.waldmannstetter@tum.de

†equal contribution

1 Introduction

The standard treatment for glioma is an *operative procedure (OP)* aiming to remove the tumor in full. Clinicians measure the success of surgery by comparing pre- and post-operative scans. Furthermore, this comparison is required for subsequent treatment planning, such as radiation therapy. Image registration techniques can enhance this process by providing a direct overlay of the differing structures. Enormous tissue shift and consequential missing correspondences mark a common side effect of tumor resection and pose a major challenge in registering pre- to post-operative images. The same holds true for intra-operative imaging in order to keep track of the surgery progress. A fast and accurate image registration method is beneficial for the precise estimation of tumor resection. Additionally, image registration is an important part of the preprocessing for segmentation algorithms [15, 16]. Moreover, registration can be part of the segmentation algorithm itself [11]. Recent advances in the field of *Deep Learning (DL)* also benefited medical image registration. Methods like *VoxelMorph (VM)* [6], *LapIRN* [19], and *TransMorph* [9] have demonstrated that unsupervised deformable image registration is a promising alternative to frameworks based on iterative optimization algorithms like *Symmetric Normalization (SyN)* from *Advanced Normalization Tools (ANTs)* [3], *Free-Form Deformation (FFD)* [21] or toolboxes like Elastix [13]. *DL* methods provide comparable performance while significantly improving processing time. Within the scope of the *Brain Tumor Sequence Registration Challenge (BraTS-Reg)* [4], there has also been considerable development of registration algorithms for MR brain images before and after tumor resection [8, 12, 17, 18, 25]. Unsupervised *Deformable Registration Network (DRN)* can nicely register healthy brain scans [6, 9, 19]; however, they frequently struggle with large pathologies. Therefore, *Instance-Specific Optimization (IO)* proved to be advantageous to mitigate major deformations [18, 25]. Existing deep learning registration algorithms usually make use of a single similarity metric, often coupled with a smoothing regularization based on the deformation field, to be optimized in the loss function [6, 19]. However, there is only limited literature investigating the combination of multiple similarity metrics to improve registration results [1, 2, 7, 10, 22, 23, 26].

In this work, we extend an unsupervised *DRN* using a combination of image similarity metrics, which are optimized simultaneously in the loss function. We benchmark the performance of our approach against the baseline on two challenging datasets of pre- to post-operative as well as pre- to intra-operative brain tumor images. Furthermore, we compare our approach to established reference methods, achieving competitive results. Following [6, 18, 25], we opt for instance-specific optimization in addition to the *DRN*. We demonstrate that the simultaneous optimization of two similarity metrics can improve registration accuracy in terms of *TRE* on expert landmark annotations.

2 Methods

Our workflow consists of three steps. First, we train a *Deformable Registration Network (DRN)*, followed by *Instance-Specific Optimization (IO)* at test time. Both *DRN* and *IO* optimize the same loss function. We then evaluate the registration performance in terms of *Target Registration Error (TRE)*.

2.1 Unsupervised Deformable Registration

We start our approach with a *DRN*, similar to [6]. Given two 3D images, a source image X and a target image Y , the network models the following function $f_\theta(X, Y) = u$, where the displacement field u , aligning X and Y , is defined bidirectionally, leading to $u_{x,y} = f_\theta(X, Y)$ and $u_{y,x} = f_\theta(Y, X)$ with θ being a set of learning parameters. X and Y are then warped with the respective displacement field using a spatial transform. While many *Convolutional Neural Network (CNN)*-based models are applicable here, like [6], we opt for a *U-Net*-like architecture with encoder, decoder and skip connections. The network architecture is based on an early implementation of *VM*, see GitHub implementation. The loss function comprises two main components, which are an image similarity metric and a smoothness regularizer for the displacement field. In addition to optimizing a single similarity metric as part of the loss function, we opt for optimizing multiple metrics simultaneously. An overview of the workflow is shown in Figure 1.

2.2 Proposed Combined Loss Function

We define the objective function L for bidirectional training as follows:

$$L = \sum_{n=1}^N \left(L_{Sim_n}^{forward} \cdot \omega_n + L_{Sim_n}^{backward} \cdot \omega_n \right) + L_{Reg} \cdot \lambda \quad (1)$$

where N is the number of similarity metrics L_{Sim} , L_{Reg} is the regularization term, and the respective weights are denoted by ω_n and λ .

2.3 Instance-specific Optimization

Since the registration results of a plain *DRN* might not always be sufficient, especially in the case of pathologies, *IO* is added in order to further refine the registration. Similar to [6], we take the output displacement field of *DRN* as initialization for a gradient-descent based iterative optimization on each test scan individually, following the initial training process. This technique optimizes the same loss function that is used for *DRN*. An overview of the complete method is given in Figure 1.

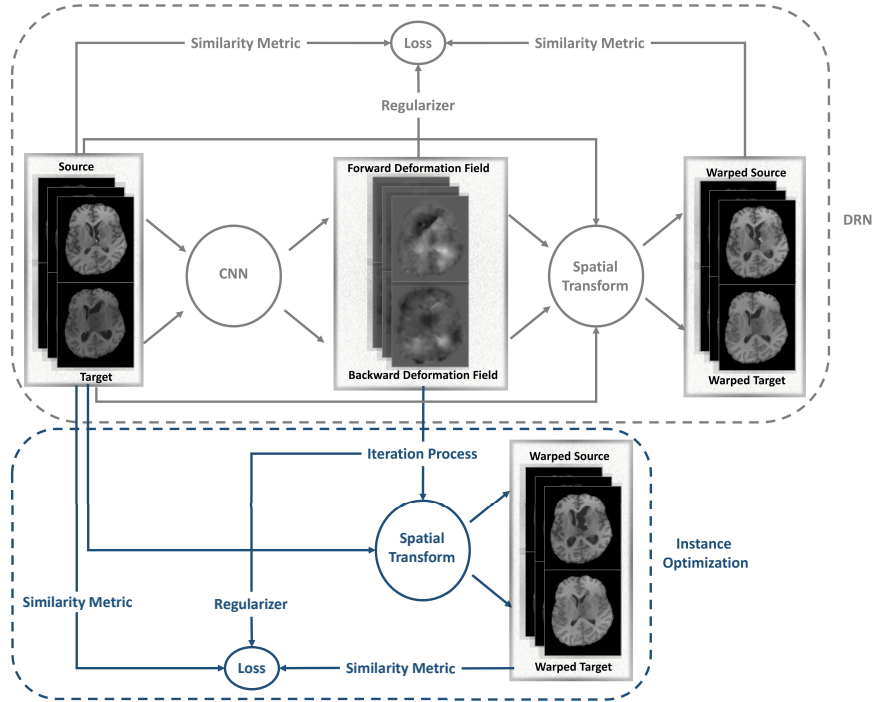


Fig. 1: Overview of the workflow. An unsupervised deformable registration network (*DRN*, top) is combined with *Instance-Specific Optimization (IO)* (bottom) for iterative refinement at test time using the output deformation field of the trained *DRN*. *DRN* as well as *IO* are trained bidirectionally, providing both forward and backward deformation fields. For both modules, the loss function combines either a single or multiple image similarity metrics with a smoothness regularization on the deformation field.

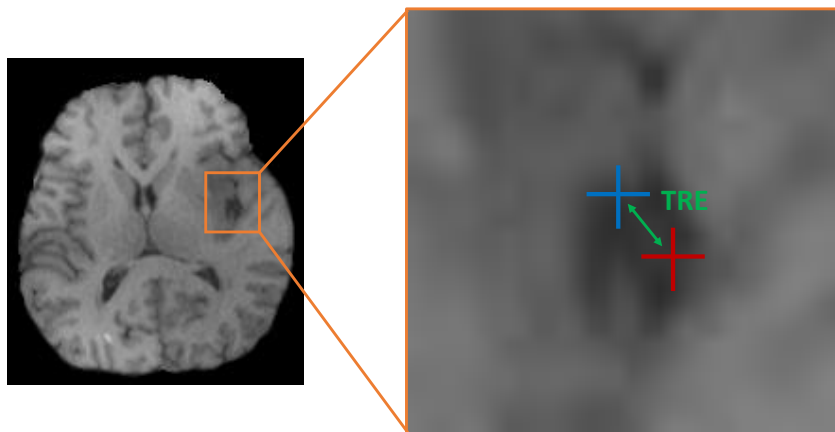


Fig. 2: Illustration of *Target Registration Error (TRE)* evaluation between expert landmark annotation (red) and warped landmark after image registration (blue). The green arrow indicates the Euclidean distance between the two points. For simplicity, the illustration is in 2D, while the actual evaluation is performed in 3D space.

2.4 Evaluation

We evaluate all experiments by calculating the mean *TRE* between the expert landmark annotations and the warped landmarks on the respective test sets. We use the Euclidean distance to calculate the *TRE*, as illustrated in Figure 2.

3 Experiments and Results

We perform experiments using different loss functions on two brain *Magnetic Resonance Imaging (MRI)* datasets. Additionally, we implement two reference methods for comparison.

3.1 Data and Pre-Processing

Training and evaluation are performed on two brain tumor datasets comprising 419 paired exams in total:

Pre-Post-OP (PP): Contains 300 pairs of brain MR exams with one timepoint before and one timepoint after tumor resection. It is comprised of the official training+validation dataset of *BraTS-Reg* [4] with 160 cases and three datasets collected at *Klinikum rechts der Isar (TUM)* with 49, 30, and 61 cases, respectively.

Pre-Intra-OP (PI): Contains 119 pairs of brain MR exams with one timepoint before and one timepoint during tumor surgery and originates again from *Klinikum rechts der Isar (TUM)*.

Each exam comprises either three or four of the MR sequences *native T1-weighted (T1)*, *contrast-enhanced T1 (T1CE)*, *T2-weighted (T2)*, *T2 Fluid Attenuated Inversion Recovery (FLAIR)*. We preprocess the data using the *BraTS toolkit* [14], which includes reorientation into the same coordinate system, rigid co-registration to a brain atlas as well as brain extraction. Additionally, intensity normalization is applied to all images. For testing, we use 30 cases for *PP* and 20 cases for *PI*. For each test set, six landmarks annotated by clinical experts are provided for each case, accumulating to 180 landmarks on 30 patients for *PP* and 120 landmarks on 20 patients for *PI*.

3.2 Similarity Metrics

We demonstrate the simultaneous optimization strategy on the similarity metrics *Mean Squared Error (MSE)* and *Normalized Cross Correlation (NCC)*, which are widely used for medical image registration tasks [6].

3.3 Training and Testing

We perform multi-channel training and testing for *DRN* and *IO*. For *PP*, this includes all four sequences, while for *PI*, the sequences *T1*, *T1CE* and *FLAIR* are available. To overcome this imbalance, we train separate networks for *PP* and *PI*. We split the *PP* dataset into training (80%), validation (10%), and test (10%) and select the model for testing that shows a minimal loss on the validation set. Since we have much fewer cases available for the experiments on the *PI* dataset, we waive the validation set here and decide on a fixed number of 600 training epochs in all experiments. At test time, the *DRN*'s output deformation field serves as input to the 30 iterations of *IO*. For each dataset, we compare the combined loss of *MSE+NCC* against the individual addends, both for the initial *DRN* training as well as the *IO*. Therefore, we exhaustively explore loss combinations for *DRN* and *IO*, as depicted in Table 1.

The implementation is inspired by [6] using *Pytorch* 1.8.1 [20]. We use learning rates $1e-4$ and $1e-3$ for *DRN* and *IO*, respectively. Image similarity metrics are weighted equally in the loss function, summing up to 1 for the similarity term. Smoothness regularization weight is set to 1.0 for all experiments for a fair comparison.

3.4 Reference Methods

We compare our approach with two established methods: a deformable *SyN* registration by *ANTs* [3], and *VM* [6], both using the respective T1-weighted sequences. We implement two variants of *VM* [6], available at [5], that employ *MSE* and *NCC* as respective image similarity metrics. Therefore, we use default learning rate $1e-4$ and recommended smoothness regularization weights of 0.02 and 1.5 for *MSE* and *NCC*, respectively. Likewise, *ANTs SyN* [3] is implemented using default parameters. Since we opt for deformable registration without prior rigid/affine alignment, we apply the same for *VM* and *ANTs SyN*.

Table 1: Mean $TREs$ in mm with standard deviation using different losses for DRN and $DRN+IO$ on the Pre-Post-OP and Pre-Intra-OP test sets. Shown are the results on all possible combinations of loss functions. The best result in each category is highlighted. Statistical comparisons are provided in Table 2. Hit rate curves [24] are shown in Figure 3.

Loss [DRN]	Loss [IO]	Pre-Post-OP	Pre-Intra-OP
MSE	(not applied)	2.40±1.56	3.48±3.45
MSE	MSE	2.21±1.56	3.27±3.46
MSE	NCC	1.81±1.45	3.24±3.39
MSE	MSE+NCC	1.76±1.36	3.17±3.39
NCC	(not applied)	2.18±1.52	3.31±2.68
NCC	MSE	2.06±1.50	2.96±2.78
NCC	NCC	1.80±1.44	2.71±2.79
NCC	MSE+NCC	1.77±1.36	2.68±2.72
MSE+NCC	(not applied)	2.19±1.49	3.07±2.96
MSE+NCC	MSE	2.07±1.48	2.94±3.05
MSE+NCC	NCC	1.80±1.44	2.86±2.95
MSE+NCC	MSE+NCC	1.73±1.34	2.76±2.89

3.5 Results

Table 1 shows quantitative results on both datasets. The $TREs$ indicate that for PP , DRN only with NCC loss achieves the lowest mean error. When coupling DRN with IO , for all possible combinations, mean TRE is always lowest when using $MSE+NCC$ loss during IO . On PI , lowest mean TRE for DRN only is achieved when combining MSE and NCC in the loss function. When adding IO , DRN with NCC loss coupled with IO using $MSE+NCC$ loss shows lowest mean TRE . Statistical comparisons based on *Paired Samples T-Tests* are provided in Table 2.

Table 2: P -values and 95% Confidence Intervals (CI) of *Paired Samples T-Tests* on the TRE of competitive methods for the Pre-Post-OP and the Pre-Intra-OP datasets. Methods are given by declaring the used losses for DRN and IO , respectively.

Method 1	Method 2	p-value [CI] (Pre-Post-OP)	p-value [CI] (Pre-Intra-OP)
DRN (NCC)	DRN (MSE+NCC)	0.85 [-0.09; 0.07]	0.05 [0.00; 0.47]
DRN (MSE) + IO (NCC)	DRN (MSE) + IO (MSE+NCC)	0.13 [-0.01; 0.10]	0.23 [-0.04; 0.16]
DRN (NCC) + IO (NCC)	DRN (NCC) + IO (MSE+NCC)	0.22 [-0.02; 0.08]	0.50 [-0.06; 0.13]
DRN (MSE+NCC) + IO (NCC)	DRN (MSE+NCC) + IO (MSE+NCC)	0.03 [0.01; 0.13]	0.03 [0.01; 0.19]

Table 3: Comparison with reference methods. Mean TRE in mm with standard deviation on the Pre-Post-OP and Pre-Intra-OP datasets for the best $DRN+IO$ compared to VM and ANTs SyN . The proposed method is on par with established reference registration methods.

Method	Pre-Post-OP	Pre-Intra-OP
DRN+IO	1.73±1.34	2.68±2.72
VM (MSE)	2.98±2.11	3.66±2.90
VM (NCC)	2.09±1.54	2.37±2.37
ANTs SyN	2.02±1.49	1.81±1.17

Moreover, we have evaluated the experiments with respect to their *hit rate* curves according to [24], see Figure 3, showing the behavior of the different methods with respect to registration accuracy with increased tolerance.

Evaluating performance with respect to running time, we determine that the runtime mainly depends on the implementation of the respective similarity metric. In our case, NCC loss is significantly slower than MSE . When combining the two metrics in the loss function, there is barely any difference in runtime compared to NCC alone, since the runtime of MSE is overall negligible. This finding will probably change when the respective implementation differs and/or other similarity metrics are used.

Table 3 shows a comparison of the best $DRN+IO$ with results achieved by reference methods VM and $ANTs$. For PP , $DRN+IO$ shows lowest mean $TREs$, while for PI , this is the case for $ANTs$ SyN .

Our findings are in line with how experts visually perceive the registration quality: In a blinded evaluation of registration methods, three expert radiologists independently picked the $MSE+NCC$ registration as their favorite. Asked to provide reasoning for their choice, experts cited better registration quality around ventricles and fewer artifacts, such as unrealistically deformed tissue. Figure 4 shows sample qualitative results on PI , illustrating these findings.

4 Discussion

The contribution of this work is to simultaneously optimize multiple image similarity metrics for image registration tasks in a DL setting. For demonstration purposes, we combine the well-established metrics MSE and NCC . We evaluate $DRNs$ with and without IO in two challenging multi-modal 3D registration settings, namely pre- to post-operative and pre- to intra-operative glioma MRI .

Table 1 shows that combining MSE and NCC losses consistently improves IO performance in both datasets. When applied to DRN only, the combination still performs best for PI while showing comparable results to NCC for PP . Furthermore, Table 3 illustrates that our method achieves competitive results compared to established reference methods. Moreover, for PP , the proposed approach outperforms all reference methods. For PI , $ANTs$ SyN performs best.

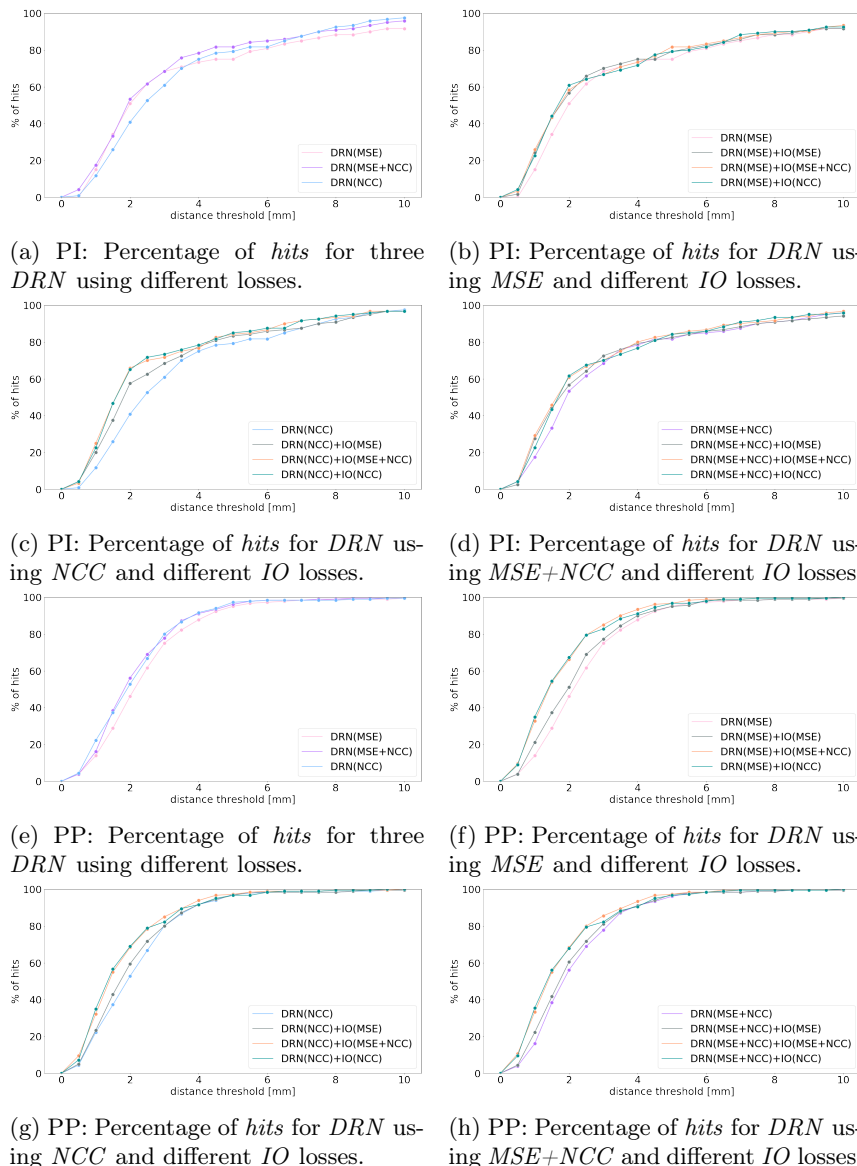


Fig. 3: Hit rate curves [24] on PI and PP, respectively. *Hit* denotes that a warped landmark lies within a certain distance threshold to the respective expert landmark annotation. Here, evaluation thresholds are set every 0.5mm, *hit* percentages in between are interpolated.

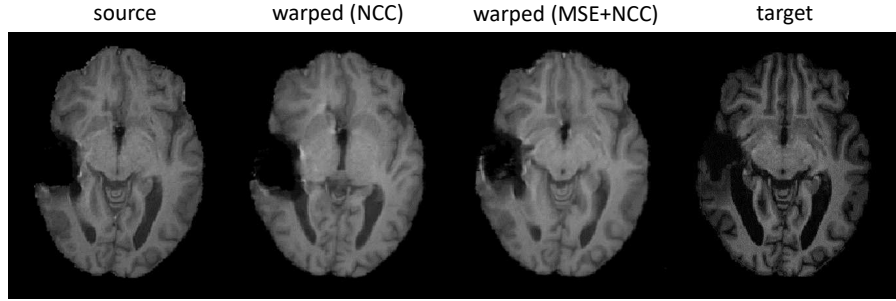


Fig. 4: Sample registration results on the Pre-Intra-OP dataset. Registration with combined losses $MSE+NCC$ shows improved registration in comparison to registration with NCC only, especially nearby the tumor and the resection cavity, respectively.

A potential explanation might be lower registration quality introduced by the *FLAIR* images. When using *T1* images only for training and testing, the results are getting more comparable, see Table S1 in the supplementary material. Also, *DRN* as well as *VM* would likely benefit from a bigger training dataset. When performing an additional experiment using the Elastix toolbox [13] for single- vs multi-metric registration, we can observe that combining two metrics improves performance for *PI*, see Table S2 in the supplementary material.

Combining MSE and NCC can help to improve the alignment of the source image to the target image. The qualitative assessment by clinical experts supports these findings.

There are several limitations to this study. The evaluation is performed on rather small test sets of 20 for *PI* and 30 for *PP*. The used datasets are fairly specific, so for generalization purposes, an extension toward other registration tasks promises to yield additional insights. Here, we focus on multi-sequence training on all available MR sequences using a 4D implementation of the NCC loss. Training on different sequences separately will possibly indicate increased understanding on the respective influences. Performing cross validation for model selection might improve stability in the results. Even though the regularization could be fine-tuned, we use a fixed weight on the deformation field in our approach.

5 Conclusion and Future Work

We propose an optimization strategy – here implemented by means of a simple summation – that benefits registration performance with regard to *TRE*. Moreover, we conduct extensive comparisons against established reference methods. Future work should investigate the addition of further similarity metrics such as *Mutual Information*. Besides, introducing different weights for the individual parts of the loss function (instead of equally weighting) might further enhance registration performance.

Acknowledgements

Supported by Deutsche Forschungsgemeinschaft (DFG) through TUM International Graduate School of Science and Engineering (IGSSE), GSC 81. BM, BW and FK are supported through the SFB 824, subproject B12. BM acknowledges support by the Helmut Horten Foundation. Finally, we acknowledge Andreas Poschenrieder and Anna Valentina Lioba Eleonora Claire Javid Mamasani for eye-opening insights.

References

1. Avants, B., Duda, J.T., Kim, J., Zhang, H., Pluta, J., Gee, J.C., Whyte, J.: Multivariate analysis of structural and diffusion imaging in traumatic brain injury. *Academic radiology* **15**(11), 1360–1375 (2008)
2. Avants, B.B., Tustison, N.J., Song, G., Cook, P.A., Klein, A., Gee, J.C.: A reproducible evaluation of ants similarity metric performance in brain image registration. *Neuroimage* **54**(3), 2033–2044 (2011)
3. Avants, B.B., Tustison, N., Song, G., et al.: Advanced normalization tools (ants). *Insight j* **2**(365), 1–35 (2009)
4. Baheti, B., Waldmannstetter, D., Chakrabarty, S., Akbari, H., Bilello, M., Wiestler, B., Schwarting, J., Calabrese, E., Rudie, J., Abidi, S., et al.: The brain tumor sequence registration challenge: establishing correspondence between pre-operative and follow-up mri scans of diffuse glioma patients. arXiv preprint arXiv:2112.06979 (2021)
5. Balakrishnan, G., Zhao, A., Sabuncu, M., Guttag, J., Dalca, A.V.: voxelmorph: Learning-based image registration, <https://github.com/voxelmorph/voxelmorph>
6. Balakrishnan, G., Zhao, A., Sabuncu, M.R., Guttag, J., Dalca, A.V.: Voxelmorph: a learning framework for deformable medical image registration. *IEEE transactions on medical imaging* **38**(8), 1788–1800 (2019)
7. Boukellouz, W., Moussaoui, A.: Evaluation of several similarity measures for deformable image registration using t1-weighted mr images of the brain. In: 2017 5th International Conference on Electrical Engineering-Boumerdes (ICEE-B). pp. 1–5. IEEE (2017)
8. Canalini, L., Klein, J., Gerken, A., Heldmann, S., Hering, A., Hahn, H.K.: Iterative method to register longitudinal mri acquisitions in neurosurgical context. In: Brainlesion: Glioma, Multiple Sclerosis, Stroke and Traumatic Brain Injuries. pp. 262–272. Springer (2023)

9. Chen, J., Frey, E.C., He, Y., Segars, W.P., Li, Y., Du, Y.: Transmorph: Transformer for unsupervised medical image registration. *Medical image analysis* **82**, 102615 (2022)
10. Ferrante, E., Dokania, P.K., Marini, R., Paragios, N.: Deformable registration through learning of context-specific metric aggregation. In: *Machine Learning in Medical Imaging: 8th International Workshop, MLMI 2017, Held in Conjunction with MICCAI 2017, Quebec City, QC, Canada, September 10, 2017, Proceedings* 8. pp. 256–265. Springer (2017)
11. Fidon, L., Aertsen, M., Kofler, F., Bink, A., David, A.L., Deprest, T., Emam, D., Guffens, F., Jakab, A., Kasprian, G., et al.: A dempster-shafer approach to trustworthy ai with application to fetal brain mri segmentation. *arXiv preprint arXiv:2204.02779* (2022)
12. Großbröhmer, C., Siebert, H., Hansen, L., Heinrich, M.P.: Employing convexadam for brats-reg. In: *Brainlesion: Glioma, Multiple Sclerosis, Stroke and Traumatic Brain Injuries*. pp. 252–261. Springer (2023)
13. Klein, S., Staring, M., Murphy, K., Viergever, M.A., Pluim, J.P.: Elastix: a toolbox for intensity-based medical image registration. *IEEE transactions on medical imaging* **29**(1), 196–205 (2009)
14. Kofler, F., Berger, C., Waldmannstetter, D., Lipkova, J., Ezhov, I., Tetteh, G., Kirschke, J., Zimmer, C., Wiestler, B., Menze, B.H.: Brats toolkit: translating brats brain tumor segmentation algorithms into clinical and scientific practice. *Frontiers in neuroscience* p. 125 (2020)
15. Kofler, F., Ezhov, I., Isensee, F., Balsiger, F., Berger, C., Koerner, M., Demiray, B., Rackerseder, J., Paetzold, J., Li, H., et al.: Are we using appropriate segmentation metrics? identifying correlates of human expert perception for cnn training beyond rolling the dice coefficient. *Machine Learning for Biomedical Imaging* **2**(May 2023 issue), 27–71 (2023)
16. Kofler, F., Shit, S., Ezhov, I., Fidon, L., Horvath, I., Al-Maskari, R., Li, H.B., Bhatia, H., Loehr, T., Piraud, M., et al.: blob loss: instance imbalance aware loss functions for semantic segmentation. In: *International Conference on Information Processing in Medical Imaging*. pp. 755–767. Springer (2023)
17. Meng, M., Bi, L., Feng, D., Kim, J.: Brain tumor sequence registration with non-iterative coarse-to-fine networks and dual deep supervision. In: *Brainlesion: Glioma, Multiple Sclerosis, Stroke and Traumatic Brain Injuries*. pp. 273–282. Springer (2023)
18. Mok, T.C., Chung, A.: Robust image registration with absent correspondences in pre-operative and follow-up brain mri scans of diffuse glioma patients. In: *Brainlesion: Glioma, Multiple Sclerosis, Stroke and Traumatic Brain Injuries*. pp. 231–240. Springer (2023)
19. Mok, T.C., Chung, A.C.: Large deformation diffeomorphic image registration with laplacian pyramid networks. In: *Medical Image Computing and Computer Assisted Intervention–MICCAI 2020: 23rd International Conference, Lima, Peru, October 4–8, 2020, Proceedings, Part III* 23. pp. 211–221. Springer (2020)
20. Paszke, A., Gross, S., Massa, F., Lerer, A., Bradbury, J., Chanan, G., Killeen, T., Lin, Z., Gimelshein, N., Antiga, L., Desmaison, A., Kopf, A., Yang, E., DeVito, Z., Raison, M., Tejani, A., Chilamkurthy, S., Steiner, B., Fang, L., Bai, J., Chintala, S.: PyTorch: An Imperative Style, High-Performance Deep Learning Library. In: Wallach, H., Larochelle, H., Beygelzimer, A., d’Alché Buc, F., Fox, E., Garnett, R. (eds.) *Advances in Neural Information Processing Systems* 32. pp. 8024–8035. Curran Associates, Inc. (2019), <http://papers.neurips.cc/paper/>

- 9015-pytorch-an-imperative-style-high-performance-deep-learning-library.pdf
21. Rueckert, D., Sonoda, L.I., Hayes, C., Hill, D.L., Leach, M.O., Hawkes, D.J.: Non-rigid registration using free-form deformations: application to breast mr images. *IEEE transactions on medical imaging* **18**(8), 712–721 (1999)
 22. Uss, M.L., Vozel, B., Abramov, S.K., Chehdi, K.: Selection of a similarity measure combination for a wide range of multimodal image registration cases. *IEEE Transactions on Geoscience and Remote Sensing* **59**(1), 60–75 (2020)
 23. Wachs, J., Stern, H., Burks, T., Alchanatis, V.: Multi-modal registration using a combined similarity measure. *Applications of Soft Computing* **52**, 159–168 (2009)
 24. Waldmannstetter, D., Wiestler, B., Schwarting, J., Ezhov, I., Metz, M., Bakas, S., Baheti, B., Chakrabarty, S., Kirschke, J.S., Heckemann, R.A., et al.: Framing image registration as a landmark detection problem for better representation of clinical relevance. *arXiv preprint arXiv:2308.01318* (2023)
 25. Wodzinski, M., Jurgas, A., Marini, N., Atzori, M., Müller, H.: Unsupervised method for intra-patient registration of brain magnetic resonance images based on objective function weighting by inverse consistency: Contribution to the brats-reg challenge. In: *Brainlesion: Glioma, Multiple Sclerosis, Stroke and Traumatic Brain Injuries*. pp. 241–251. Springer (2023)
 26. Zhou, J., Liu, Q.: A combined similarity measure for multimodal image registration. In: *2015 IEEE International Conference on Imaging Systems and Techniques (IST)*. pp. 1–5. IEEE (2015)

Supplementary Material

Table S1: Mean TRE in mm with standard deviation using different losses for DRN and $DRN+IO$ on the Pre-Intra-OP test set. For training and testing, only $T1$ images are used here.

Loss [DRN]	Loss [IO]	Pre-Intra-OP
NCC	(not applied)	2.54±2.38
NCC	NCC	1.98±2.02
NCC	MSE+NCC	1.98±2.10
MSE+NCC	(not applied)	2.63±2.75
MSE+NCC	NCC	2.21±2.38
MSE+NCC	MSE+NCC	2.18±2.33

Table S2: Mean TRE in mm with standard deviation on the Pre-Post-OP and Pre-Intra-OP datasets for single- and multi-metric registration using the Elastix toolkit. MS denotes mean squares similarity metric, while CC denotes cross-correlation similarity metric. For *multi-metric*, MS and CC are combined.

Similarity Metric	Pre-Post-OP	Pre-Intra-OP
MS	11.45±13.61	7.91±10.18
CC	2.83±2.29	2.84±2.42
multi-metric	2.89±2.34	2.72±2.07